



# Effect and mechanism of Cr deposition in cathode current collecting layer on cell performance inside stack for planar solid oxide fuel cells



Wanbing Guan, Le Jin, Wei Wu, Yifeng Zheng, Guoliang Wang, Wei Guo Wang\*

Ningbo Institute of Material Technology & Engineering, Chinese Academy of Sciences, 519 Zhuangshi Road, Ningbo 315201, China

## HIGHLIGHTS

- MOPD of the unit cell decreases or is independent of Cr in CCCL.
- Degradation of the unit cell increases or is independent of Cr in CCCL.
- Degradation of the repeating unit increases with increasing Cr content in CCCL.
- Cr affects the cell degradation, and has no influence on contact resistance.
- Cell degradation is mainly dependent on the ohmic resistance.

## ARTICLE INFO

### Article history:

Received 11 April 2013  
 Received in revised form  
 1 June 2013  
 Accepted 18 June 2013  
 Available online 27 June 2013

### Keywords:

Chromium poisoning  
 Power density  
 Degradation rate  
 Stack  
 Solid oxide fuel cell

## ABSTRACT

Quantitative effect and mechanism of Cr on cell performance inside stack are investigated by incorporating Cr in the cathode current-collecting layer (CCCL). The results show that the maximum output power density (MOPD) of the unit cell inside a stack decreases as the Cr content increases beyond  $253.81 \mu\text{g cm}^{-2}$ . The MOPD is independent of Cr when its content is less than  $253.81 \mu\text{g cm}^{-2}$  at the original operation stage. The degradation of the repeating unit inside the stack increases with increasing Cr content. When the Cr content is higher than  $182.22 \mu\text{g cm}^{-2}$ , cell degradation increases. However, cell degradation is independent of Cr content when its content is less than  $182.22 \mu\text{g cm}^{-2}$ . The addition of Cr to the CCCL increases the ohmic resistance of the CCCL and the contact between the cathode and the electrode during the initial stage. The effect of Cr on cell degradation increases with time, but Cr content has no influence on the contact resistance between the interconnect and the cathode. Cell degradation is mainly dependent on ohmic resistance, and is independent of polarization resistance. Therefore, the addition of Cr to the CCCL increases the cell ohmic resistance, but does not affect cell polarization resistance.

© 2013 Elsevier B.V. All rights reserved.

## 1. Introduction

Solid oxide fuel cells (SOFCs) have become a potential low-cost power generation technology due to their unique advantages, such as high-efficiency, having a non-noble metal catalyst in the electrode material, and being internal reforming fuel cells [1]. For commercialization of SOFC systems, they should reach 40,000 h operation time [2]. Ni–YSZ [3] and LSM–YSZ [4] are widely used as anode and cathode raw materials, respectively, for anode-supported SOFCs. For these traditional electrode materials, cathode poisoning by Cr, introduced during evaporation from metal alloys, is a main cause of cell performance [5]. Hence, the surface of Fe–Cr alloy as a metal interconnect, one of the most important

components in the SOFC stack, must be coated to prevent Cr evaporation leading to the poisoning of the cell cathode [6,7]. Applying a coating on the interconnect can protect the metal alloy from high-temperature oxidation and prevent Cr evaporation. Currently, a large number of high-temperature alloys containing Cr are used in the SOFC system hot box, including the heat exchanger, carburetor, burner, and gas tube [8]. At the high temperatures in the hot box, Cr in the SOFC system inevitably evaporates and is deposited on in the cathode as a result of high-speed gas flow, causing cell performance degradation.

To address this challenge, researchers have been diligently investigating the mechanism of Cr poisoning and how it affects cell performance, and have made significant progress [9–15]. The researchers realize the necessity for quantitative determination of the content and the distribution of Cr in the cathode, and develop methods for its measurement [16–18]. However, measuring the content and the distribution of Cr in the cathode side is difficult due

\* Corresponding author. Tel.: +86 574 8791 1363.  
 E-mail address: [wgwang@nimte.ac.cn](mailto:wgwang@nimte.ac.cn) (W.G. Wang).

to the complex operational environment of the SOFC, which is characterized by high temperature and high-speed flowing gas, among other factors. Some researchers have found that the evaporation rate of Cr is not equal to its deposition rate in the cell cathode and that the Cr distribution in the cathode is not uniform [19,20]. As a result, of these uncertainties regarding the presence and behavior of Cr in the cathode, it is difficult to verify the operating mechanism and the correlation between cell performance and the amount of Cr. Nevertheless, a few results have been obtained regarding the prediction of the influence of Cr on cell performance [6,19,21]. However, no clear relationship between Cr content and the cell performance inside an SOFC stack has been established, because many complex factors affect cell performance [20,22,23]. In 2012, Horita et al. [24] obtained the first correlation between cell performance and Cr content in the cathode by adding Cr into an LSM cathode. However, that research focused on the oxidized Cr/Pt-mesh/cathode/GDC/Pt-paste-Pt-mesh, which is considerably different from an actual SOFC stack and with the operating conditions.

The quantitative effect of Cr on cell performance during the actual stack operation is not found until now. However, the mechanism of Cr affects cell performance by poisoning the cathode has been widely reported [25–31]. The mechanism can be summarized as follows: Cr poisons the cell cathode in the triple-phase boundary, resulting in an increase in the polarization resistance of the cathode. An electrochemical reaction model, a chemical reaction model, and a physical model of Cr poisoning have each been established and demonstrated [32]. Recently, it was found that Cr deposition in a porous cathode causes serious deterioration in cell performance under open-circuit voltage (OCV) conditions for SOFCs, seemingly verifying the mechanisms of the chemical reaction model and the physical model of Cr poisoning of the cathode [33]. However, Cr poisoning mechanisms of the three models in the cathode side mentioned above may exist simultaneously, and affect cell performance during actual stack operation due to the complex operating environment. Therefore, the mechanism of Cr affecting cell performance by poisoning the cathode must be further studied and verified to reach a greater level of understanding.

Overall, the quantitative correlation between the amount of Cr and cell performance has not been determined for actual SOFC stack operation due to the difficulty in determining Cr content and its distribution in the cathode. The mechanism of Cr affects cell performance is yet to be verified and confirmed. In this study, the quantitative effect of Cr on cell performance is measured and the mechanism by which Cr affects cell performance is examined by investigating cell performance through incorporation of Cr into the cathode current-collecting layer (CCCL) during actual stack operation.

## 2. Experimental

In this study, anode-supported Ni–YSZ/YSZ/LSM–YSZ and commercial ferritic stainless steel SUS 430 were used as the unit cell and metal interconnect, respectively. The size of a cell inside the stack is 10 cm × 10 cm with an active area of 63 cm<sup>2</sup>. Other parameters are indicated in our previously published report [34]. The structure of the gas channel on the anode side of the metal interconnect was formed along the regular line groove by the erosion etching method. A metal mesh was welded on the interconnect as the oxidized gas channel and cathode current collector. The Ni–Cr/LSM composite coating was applied using plasma spraying technology onto the cathode surface of the metal interconnect to protect it from deposition of vaporized Cr and to prevent the reduction in stack performance during operation under high temperature. The coating process and the microstructure of the Ni–

Cr/LSM composite coating are also described in our previous work [23]. A description of the performance of the Al<sub>2</sub>O<sub>3</sub>–SiO<sub>2</sub>–CaO-based glass sealing component can be found in our previous literature [35].

The anode current-collecting layer, a 130 μm–150 μm thick coating of NiO was applied to the cell anode by screen printing. A 100 μm thick layer of porous nickel was pasted on the anode side of the metal interconnect during the assembly of the stack to enhance the anode current collection. An approximately 250 μm thick layer with the composition of (La<sub>0.75</sub>Sr<sub>0.25</sub>)<sub>0.95</sub>MnO<sub>3</sub> (LSM) was printed on the cell as the CCCL. In this study, in order to measure the quantitative effects of Cr on cell performance by poisoning the cathode, various amounts of Cr were introduced into the LSM current-collecting slurry. Specifically, the cathode current-collecting slurry (CCCS) was mixed with Cr and LSM powders as raw materials. The nominal contents of Cr in the CCCS were 0, 0.1, 0.3, 0.5, 1.0, 1.5, and 3 wt. %. The actual content of Cr in the CCCS, determined by using an ICP-AES (Perkin–Elmer Optima 2100 model) apparatus, was 0, 0.13, 0.28, 0.41, 0.96, 1.21, and 2.61 wt. %. The overall quality of the CCCS for each cell was 3.9, 4.0, 4.1, 3.9, 4.1, 3.9, and 4.0 g, with a corresponding Cr quality of 0, 0.0052, 0.01148, 0.01599, 0.03936, 0.04719, and 0.1044 g. That is, the corresponding quality of Cr in the effective area was 0, 82.54, 182.22, 253.81, 629.05, 749.05, and 1657.14 μg cm<sup>-2</sup>, respectively.

To investigate the quantitative effect of Cr on cell performance, a seven-cell stack (called stack 1) was assembled according to the structure shown in Fig. 1 [36]. The units cells were labeled with numbers 1–7 in increasing order of Cr content: Cell 1 had the lowest Cr content and Cell 7 the highest. A voltage lead was placed on the surface of the current-collecting layer on each of the two sides of the unit cells during the stack assembling process, as shown in Fig. 2. The cell voltage can be detected in real time to obtain the power density variation and degradation of the stack performance, as well as of each repeating unit and unit cell, through the voltage leads. In Fig. 2, the voltage between leads 1 and 2, 3 and 4, 5 and 6, 7 and 8, 9 and 10, 11 and 12, and 13 and 14 denotes the voltage of each of the unit cells, and the voltage between leads 1 and 3, 3 and 5, 5 and 7, 7 and 9, 9 and 11, 11 and 13, and 13 and 15 denotes the voltage of each of the repeating units (each repeating unit contains one interconnect and one unit cell).

After assembly, the stack was placed into a furnace, and heated at a rate of about 1 °C min<sup>-1</sup> to 850 °C. In order to ensure proper sealing effect, a pressure of approximately 10 N cm<sup>-2</sup> of the

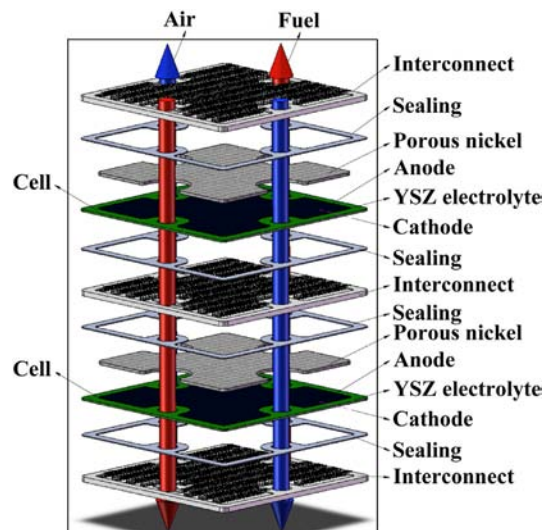


Fig. 1. Schematic diagram of stack assembling structure.

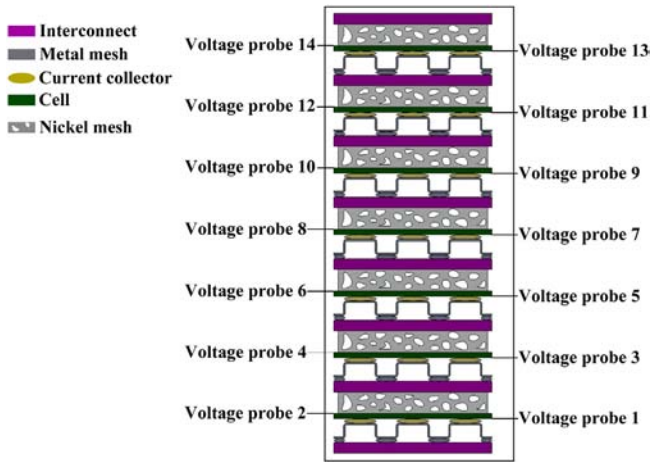


Fig. 2. Schematic diagram of voltage lead arranged inside stack.

pressure was applied on the stack. Subsequently, the stack temperature was reduced to 800 °C followed by performance measurement. Nitrogen (N<sub>2</sub>) gas was fed into the anode at a flow rate of 1 SLM for about 10 min, and then hydrogen (H<sub>2</sub>) with 3% humidity and air were fed into the cell anode and cathode, respectively. After reduction of the anode for more than 3 h, the curves of the current–voltage (*I–V*) and degradation were measured. The cell microstructure was subsequently characterized using scanning electron microscopy (SEM, Hitachi S–4800).

In order to investigate the mechanism of Cr on cell performance, a vastly increased amount of Cr compared to the above experiments needed to be added into the CCCS. Therefore, 30 wt. % Cr was introduced into the CCCL of a unit cell (unit cell 2 in the stack), and then unit cell 2 was assembled into a two-cell stack (named stack 2) with another cell (unit cell 1) in which the CCCL had no Cr, according to the schematic diagram shown in Fig. 1. Electrochemical impedance spectra (EIS) were recorded by using a frequency response analyzer (FRA, Solartron 1260/1287) to obtain the ohmic and polarization resistance of the unit cell and of the repeating unit inside the stack at set intervals during operation. In order to quantitatively analyze the resistance source of different parts of the unit cell, the voltage lead was arranged according to the schematic diagram shown in Fig. 3. The voltage lead arranged on the cell surface, as shown in Fig. 3, is slightly different from that shown in Fig. 2. The voltage lead was arranged on the electrode surface of the unit cell and on the gas channel of the interconnect to measure the voltage between various locations, to identify Cr on the resistance source of various parts of the repeating unit inside the stack. A sealing component was applied to isolate the voltage lead and the

metal–interconnect to avoid their direct contact, which can result in a short circuit.

### 3. Results and discussion

#### 3.1. Influence of Cr on performance of unit cell and of repeating unit inside stack

Fig. 4 shows the current–voltage (*I–V*) curve of the stack and the corresponding repeating unit and unit cell. The OCV of this seven-cell stack (stack 1) reaches 8.076 V at 800 °C under the gas flow rate of H<sub>2</sub>/Air = 6.8/20.4 sccm cm<sup>–2</sup>. The average OCV of the unit cell is 1.153 V. According to the Nernst equation, the voltage in our experimental condition is about 1.09 V, which is consistent with that reported in our group’s previous publication [37]. The experimental value is a little higher than the theoretical sealing value for our experimental condition, implying an excellent sealing performance. The maximum output power density (MOPD) of this stack is 0.396 W cm<sup>–2</sup> with a corresponding output power and fuel utilization of 174.597 W and 62%, respectively. The MOPDs of repeating units 1–7 inside this stack are 0.419, 0.361, 0.403, 0.418, 0.406, 0.399, and 0.362 W cm<sup>–2</sup>, respectively. The corresponding MOPDs of the unit cell are 0.429, 0.374, 0.432, 0.431, 0.418, 0.415, and 0.382 W cm<sup>–2</sup>, respectively.

The correlation between Cr content and the MOPD of the unit cell and of the repeating unit is shown in Fig. 5. The MOPD of the unit cell and of the repeating unit decreases with an increasing content of Cr when the Cr content is more than 253.81 μg cm<sup>–2</sup>. The MOPD of the unit cell reaches 0.431 and 0.432 W cm<sup>–2</sup> with Cr content of 182.22 and 253.81 μg cm<sup>–2</sup>, respectively, while the MOPD of the unit cell without Cr in the CCCL is 0.429 W cm<sup>–2</sup>. The performance of the former (unit cell with Cr) is slightly higher than that of the latter (unit cell without Cr). In contrast, the MOPD of the repeating unit is lower than that of the unit cell without Cr in the CCCL (as shown in Fig. 5), implying that Cr in the CCCL increases the interfacial contact resistance between the interconnect and the electrode during the initial stage of stack operation. Accordingly, repeating unit 2 has the lowest MOPD among all repeating units, which may be due to the low performance of the unit cell itself. The results imply that Cr content has no influence on the MOPD of a unit cell inside the stack, since Cr content is less than 253.81 μg cm<sup>–2</sup> at the original operation stage.

The differences in the voltage drop Δ*U*<sub>IC</sub> caused by the unit cell and by the repeating unit were calculated, and the results are presented in Fig. 6a). The voltage drop Δ*U*<sub>IC</sub> between the unit cell and the repeating unit has a linear relationship with the corresponding current density. The slope of the line can be obtained by fitting the voltage drop difference curve, denoting the resistance *R*<sub>IC</sub> source of the metal interconnect and the interfacial contact

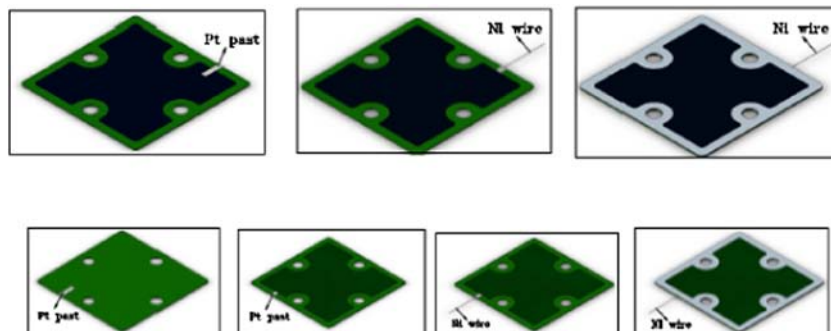


Fig. 3. Schematic diagram of voltage probe arranged on both sides of unit cell.

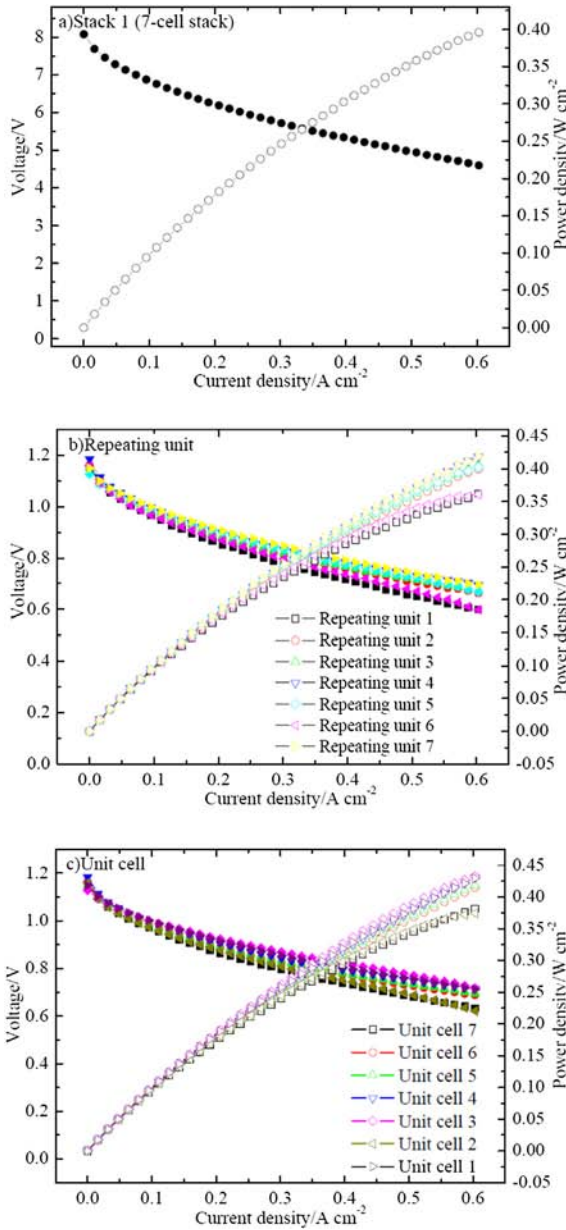


Fig. 4. *I*–*V* curve of stack and its corresponding repeating unit and unit cell at 800 °C: a) stack 1, b) repeating unit, c) unit cell.

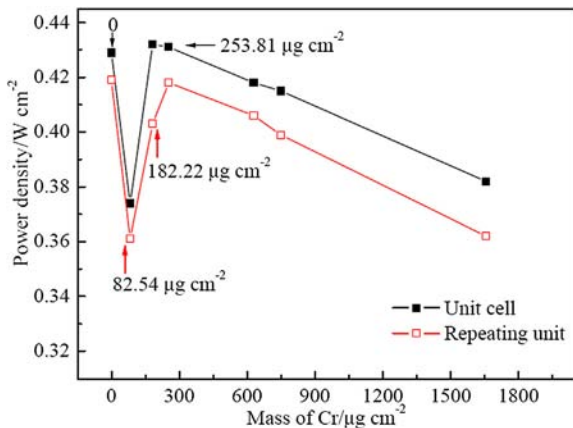


Fig. 5. The correction of Cr and power density of unit cell and repeating unit.

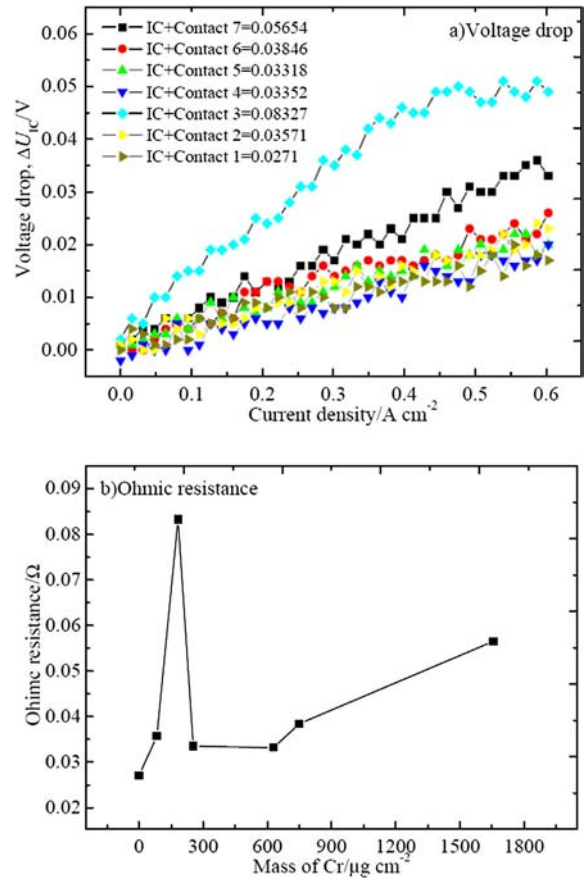


Fig. 6. The relationship between the content of Cr and the resistance source of the interfacial contact and the interconnect: a) voltage drop, b) ohmic resistance.

between the cathode and the interconnect. The relationship between the resistance  $R_{IC}$  and Cr content is shown in Fig. 6b). As shown in this figure, the resistance  $R_{IC}$  increases with the increasing Cr content in the CCCL. The resistance  $R_{IC}$  of unit cell 3 increases significantly compared with those of other unit cells, which may be due to an improper electrical interfacial contact of the corresponding repeating unit or by an improper connection of probe 7 with the corresponding interconnect (as seen in Fig. 2).

After stack disassembly, a clear and uniform contact is found on the CCCL of unit cells 1 to 7, and the representative morphology of their traces is illustrated in Fig. 7a) and b). Accordingly, the interfacial contact between the cathode and the interconnect is not a major factor in the stack performance, based on the findings of our previous studies [23,38]. Therefore, it can be concluded that the change in power density of the repeating unit in the stack is mainly caused by Cr, and the performance of repeating unit 2, having the

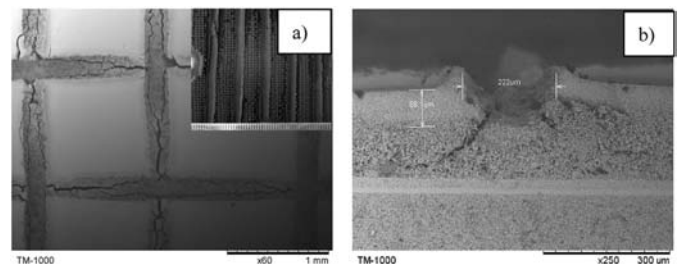


Fig. 7. Representative morphology of trace left on the CCCL after stack disassembly: a) surface morphology, b) cross section.

lowest value compared with the other units, results primarily from poor cell performance. Similarly, it can be deduced that the repeating unit 3's highest  $R_{IC}$  is perhaps mainly caused by probe 7's poor connection with its adjacent interconnect.

Fig. 8 shows the degradation curves of the stack and the corresponding repeating unit and unit cell at the current density of  $0.508 \text{ A cm}^{-2}$ . The original operation voltage of the stack is  $4.96 \text{ V}$  (i.e., the average operation voltage of each unit cell is approximately  $0.7 \text{ V}$ ) with a corresponding power and fuel utilization of  $159 \text{ W}$  and  $52\%$ , respectively. The degradation rate of the stack is  $1.06\%$  per  $100 \text{ h}$  during the  $460\text{-h}$  operation. The OCV of the stack reaches  $8.1, 8.07, 8.07,$  and  $8.3 \text{ V}$  when the stack operates for  $5, 95, 405,$  and  $458 \text{ h}$ , respectively. The results show that the stack has an excellent sealing performance throughout the whole operation, indicating that sealing is not a factor in cell degradation. The degradation rates of unit cells 1 to 7 are  $0.12\%, 0, 0.38\%, 0.62\%, 0.76\%, 5.0\%$ , and  $5.9\%$ , respectively, per  $100 \text{ h}$  with the degradation rates of the

corresponding repeating units being  $0.006\%, 0.32\%, 0.02\%, 0.26\%, 0.65\%, 1.5\%$ , and  $4.56\%$  per  $100 \text{ h}$ , as shown in Fig. 8b) and c). Therefore, we conclude that the degradation rate of the repeating unit increases with increasing Cr content except for repeating unit 2, as shown in Fig. 9. When the Cr content is less than  $182.22 \mu\text{g cm}^{-2}$ , Cr in the CCCL seemingly has no influence on the degradation of the unit cell inside the stack. When the Cr content is more than  $182.22 \mu\text{g cm}^{-2}$ , the degradation rate of the unit cell also increases with increasing Cr content. The degradation rate of the repeating unit is less than that of its corresponding unit cell, perhaps due to the improved contact during operation.

The relationship between the degradation rate of the unit cell and of the repeating unit at different operation times and Cr content is shown in Fig. 10. The degradation rates of the unit cell and of the repeating unit inside the stack decrease gradually and finally reach a constant value with increasing operation time. Compared to the corresponding unit cell, the repeating unit has a higher degradation rate within a  $72\text{-h}$  operation time, but lower degradation rate when the operation time is longer than  $72 \text{ h}$  Fig. 11 shows the area specific resistance (ASR) caused by the interconnect and by the contact between the cathode and the interconnect. The results indicate that the ASR caused by the interconnect and by its corresponding contact with the cell cathode of repeating units 1 to 7 inside the stack decreases within a  $200 \text{ h}$  operation, except for repeating unit 2 ( $0.13 \text{ wt.}\% \text{ Cr}$ ), and then remains stable after  $200 \text{ h}$ . Similar values are found for the ASR source of the interconnect and of the contact. Therefore, the results shown in Fig. 10 are probably due to the improved contact between the cathodes and the interconnects and the constant influence of Cr on cell performance with increasing operation time. At the initial operation stage, the effect of the contact generated from the interconnects and their contact with the cell cathode is dominant over the effect of Cr on cell performance by poisoning the cathode. When the stack is operated for a specific time, the improvement of the contact between the interconnects and the cathodes reaches the highest level. The improved contact and the Cr content have similar influence on cell performance, and the effect of the two factors is balanced. Finally, the degradation of the unit cell and of the repeating unit inside the stack tends to be stable.

### 3.2. Mechanism of Cr on performance of unit cell and repeating unit inside stack

The surface morphology on the cathode side of unit cells was characterized after the testing of stack 2, as shown in Fig. 12. Clear

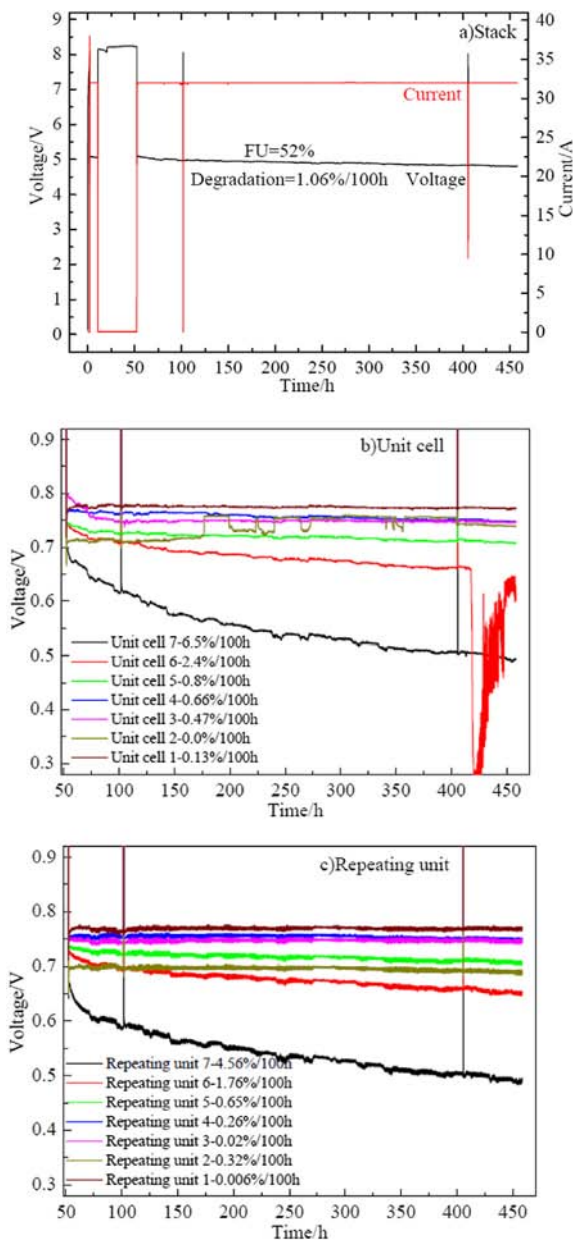


Fig. 8. The degradation curve of the repeat unit and of the unit cell at  $800^\circ\text{C}$ : a) stack, b) unit cell and c) repeating unit.

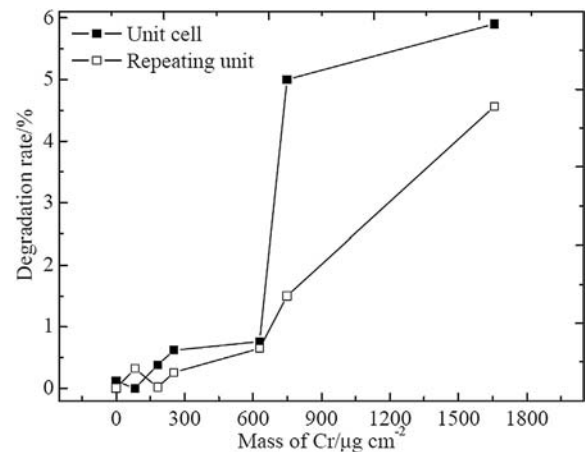


Fig. 9. The correlation between the degradation rate of the unit cell and of the repeat unit inside the stack and Cr content.

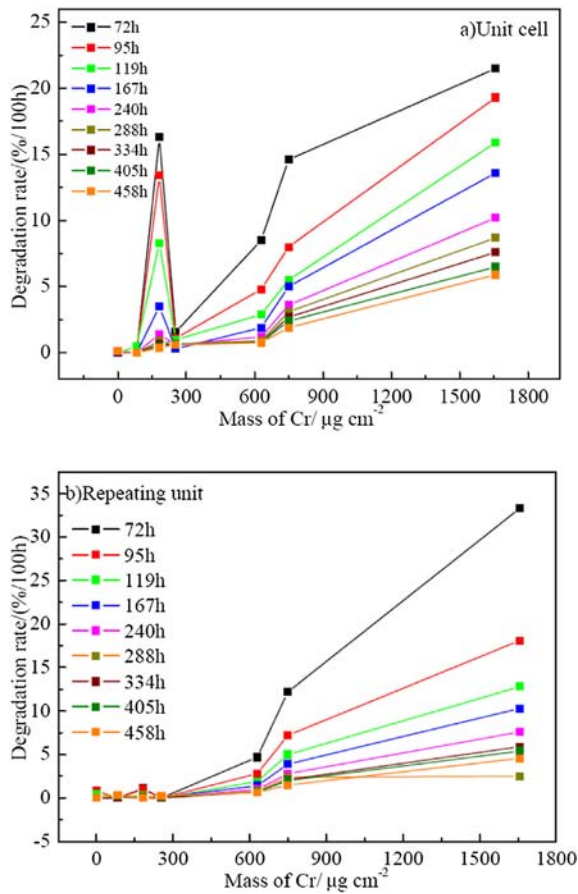


Fig. 10. The relationship between the degradation rate of the unit cell and of the repeating unit during different operation time and the content of Cr: a) unit cell, b) repeating unit.

traces are left on the cathode side of both cells. Accordingly, the performances of the unit cell and of the repeating unit inside the stack are independent of the contact between the electrode and the cell cathode, but are mainly dependent on Cr, as found in our previous research [23,38].

Fig. 13 demonstrates the *I*–*V* curves of the stack and of the corresponding unit cells with a Cr content of 0 (unit cell 1) and 30 wt. % (unit cell 2) under different operation times at 800 °C. The results show that the OCVs of the stack, unit cell 1, and unit cell 2 are 2.409, 1.201, and 1.204 V, respectively, with a gas flow rate of H<sub>2</sub>/Air = 7.9/23 sccm cm<sup>-2</sup>. The value of the OCV also indicates an

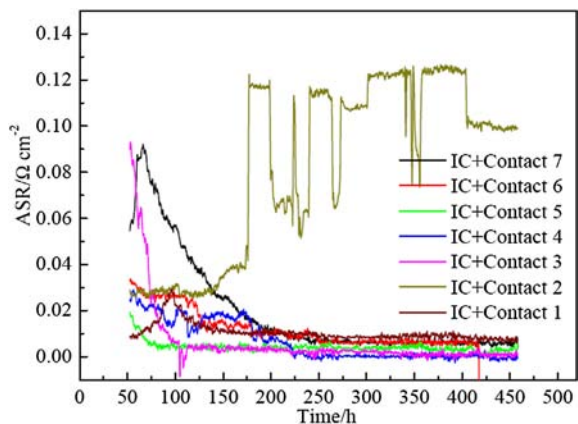


Fig. 11. The ASR source of the interconnect and of the interfacial contact.

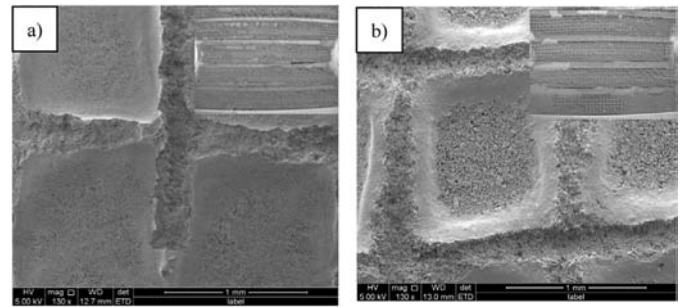


Fig. 12. Surface morphology on the cathode side of unit cells: a) unit cell 1, b) unit cell 2.

excellent sealing performance according to the value calculated using the Nernst equation. The MOPD of the stack reaches 0.388 W cm<sup>-2</sup> with corresponding power and fuel utilization of 48.9 W and 53.2%, respectively. The MOPDs of unit cells 1 and 2

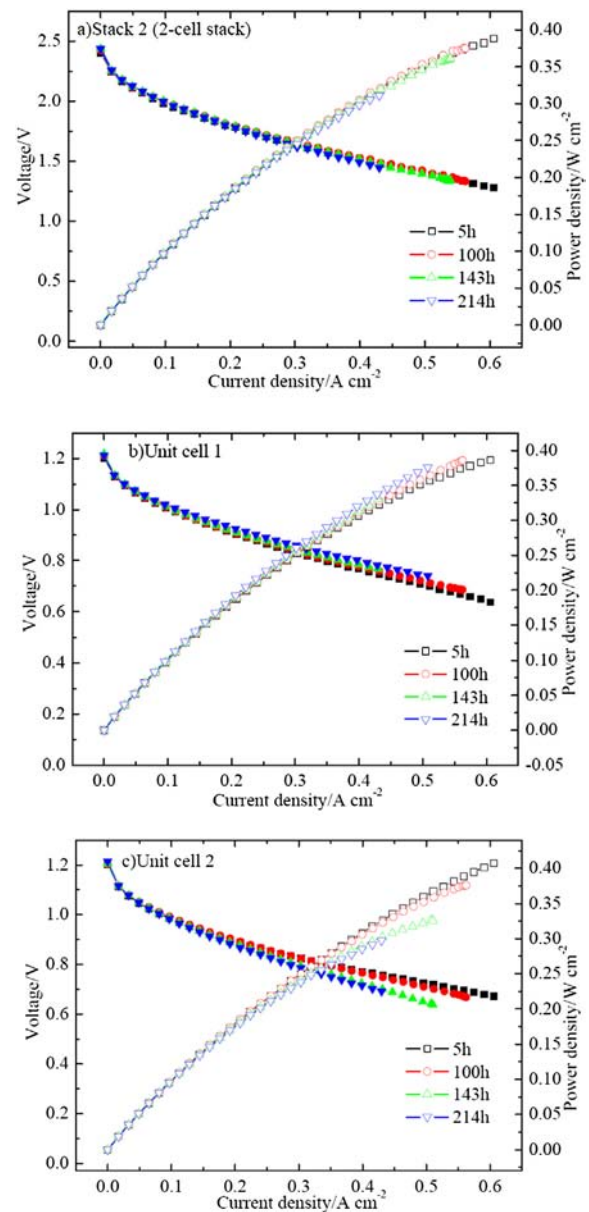


Fig. 13. *I*–*V* curves of the stack and unit cells at different operation times at 800 °C: a) stack 2, b) unit cell 1 and c) unit cell 2–30 wt. % Cr.

reach 0.386 and 0.407 W cm<sup>-2</sup>, respectively. The MOPD of unit cell 1 and its corresponding repeating unit remains stable within the 214-h operation time, while the MOPDs of unit cell 2 and its corresponding repeating unit decrease gradually.

The results shown in Fig. 13 indicate that Cr has no influence on the original performance of unit cells. So, the results of Cr's effect on cell performance obtained in the experiment and those shown in Fig. 5 seemingly contradict each other. Unlike for the two results discussed above, the content of Cr for results shown in Fig. 5 is between 0 and 1657.14 μg cm<sup>-2</sup>. When the content of Cr increases to 30 wt. %, the amount of Cr reaches 19047.62 μg cm<sup>-2</sup>, 11.5 times more than the maximum value for results shown in Fig. 5. The conductivity of the LSM applied as the CCCL is 200 S cm<sup>-1</sup> [39]. The initial phase of Cr in the CCCL appears as pure metal Cr, and the conductivity of the mixed CCCL of 30 wt. % Cr is higher than that of the pure LSM. Therefore, when the content of Cr becomes greater than a certain value, the high conductivity of the mixed CCCL with Cr plays a positive role, thereby resulting in an abnormal phenomenon whereby cell performance is improved by the elemental Cr. However, the negative effect of Cr on cell performance appears gradually with an increase in operation time. The MOPD of unit cell 2, with high Cr content in the corresponding CCCL, is evidently lower than that of unit cell 1. At this operation time, the negative effect of Cr on cell performance exceeds its positive effect observed at the initial stage.

Fig. 14 shows the I–V curves of the repeating unit inside the stack during different operation times. The results indicate that the MOPD of repeating unit 1 remains stable, while the MOPD of repeating unit 2 decreases clearly with increasing operation time. The difference in the voltage drop between the unit cell and the repeating unit is calculated, and the result is shown in Fig. 15. The

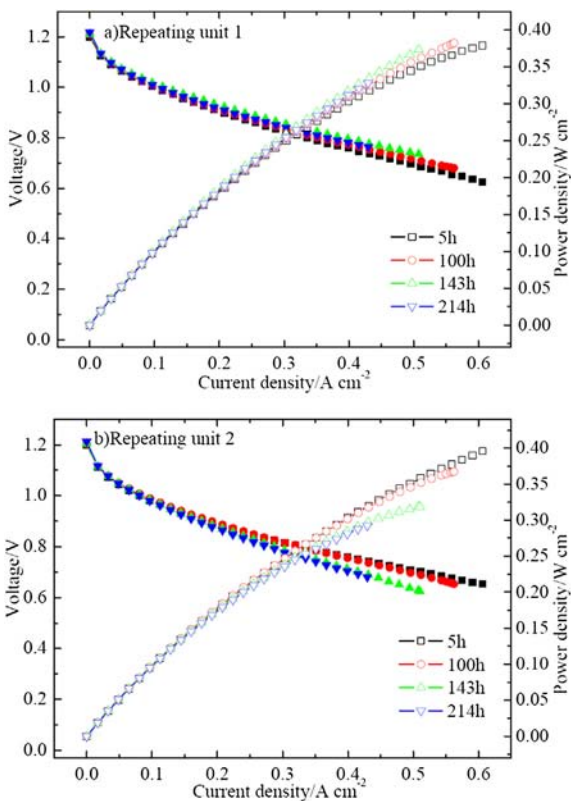


Fig. 14. I–V curves of the stack during different operation stage at 800 °C: a) repeating unit 1, b) repeating unit 2.

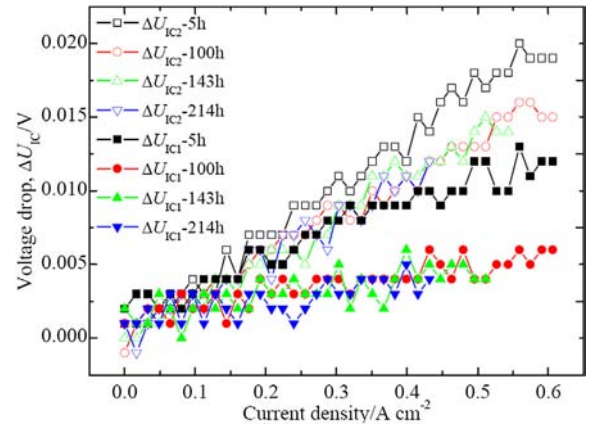


Fig. 15. The voltage drop between the repeating unit and the unit cell at different operation times.

difference in the voltage drop remains unchanged with increasing discharging current under different operation stage, that is, the resistance source of the interconnect and of the contact between the interconnect and the cell cathode shows no clear change with increasing operation time. The results indicate that the influence of Cr in the CCCL on contact resistance does not change with a change in operation time. However, the addition of Cr in the CCCL does reduce cell performance with increasing operation time. The reduced voltage drop in repeating unit 2, which is significantly larger than that of repeating unit 1 (as shown in Fig. 15), implies that the introduction of Cr in the CCCL increases the resistance of the contact and of the CCCL during the initial operation stage.

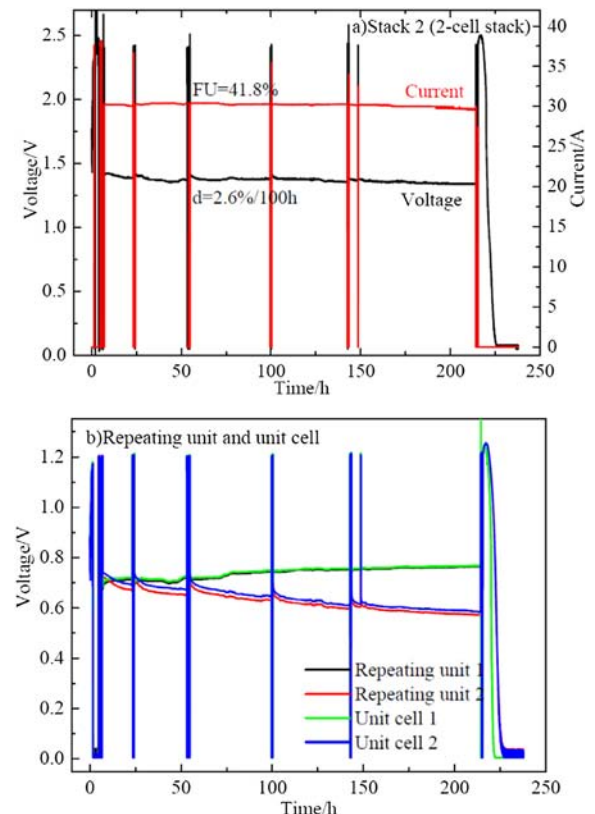


Fig. 16. The degradation rate of the stack and the corresponding repeating unit and unit cell at 800 °C: a) stack 2, b) repeating unit and unit cell.

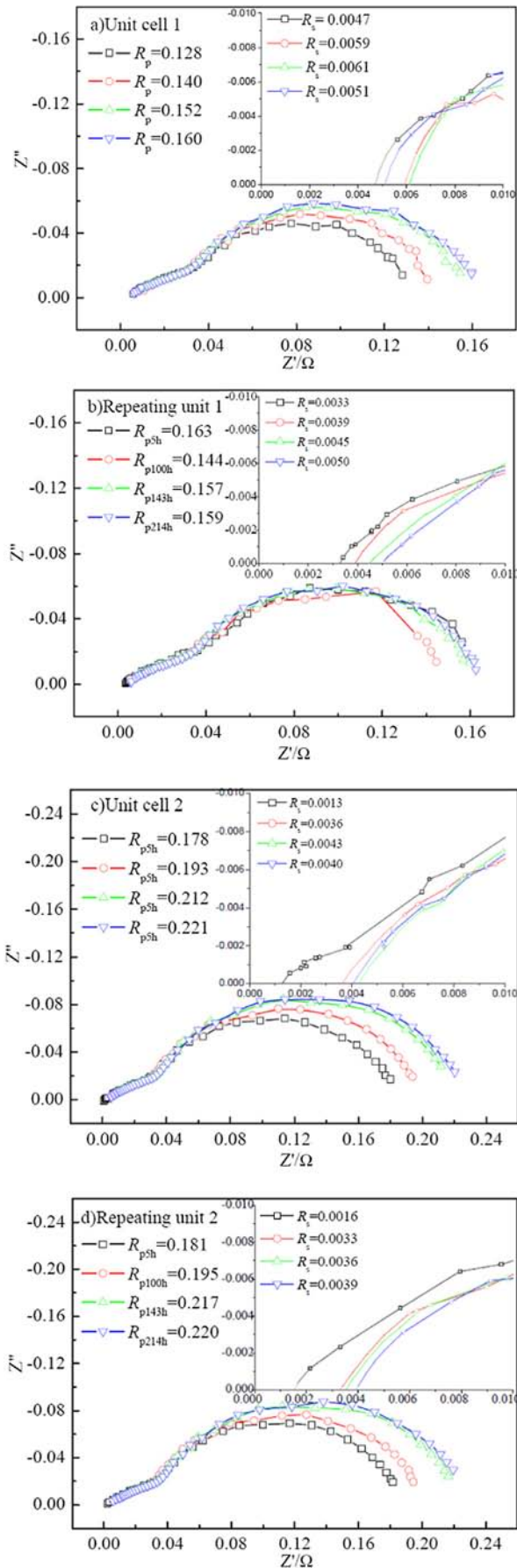


Fig. 17. EIS of the unit cell and of the repeating unit inside the stack during operation at 800 °C: a) unit cell 1, b) repeating unit 1, c) unit cell 2, and d) repeating unit 2.

Although, the resistance of the contact and of the CCCL remains subsequently unchanged, the resistance of the contact and of the CCCL source of repeating unit 2 with Cr is three times more than that of repeating unit 1 without Cr.

Fig. 16 shows the degradation curve of the unit cell and the stack. The results indicate that the original operation voltages of the stack and of the unit cells 1 and 2 are 1.407, 0.686, and 0.744 V, respectively at a discharging current density of  $0.476 \text{ A cm}^{-2}$  (with current of 30 A) under the temperature of 800 °C and the gas flow rate of  $\text{H}_2/\text{Air} = 7.9/23.8 \text{ sccm cm}^{-2}$ . The operation voltages of the corresponding repeating units 1 and 2 reach 0.767 and 0.729 V, respectively. The total degradation rate of the stack is 2.6% per 100 h after 214-h operation. The operation voltages of repeating unit 1 and unit cell 1 inside the stack exhibit no degradation, and tend to increase. However, the operation voltages of repeating unit 2 and unit cell 2 are obviously reduced, and the degradation rate reaches 7.09% per 100 h. Therefore, Cr in the CCCL significantly affects cell degradation.

Fig. 17 demonstrates the EIS measurements of the unit cell and the repeating unit inside the stack during different operation stages at 800 °C. From the figure, it can be seen that the polarization resistances of unit cell 1 and repeating unit 1 are always smaller than those of unit cell 2 and repeating unit 2, while the ohmic resistances of unit cell 1 and repeating unit 1 are always higher than those of unit cell 2 and repeating unit 2. The resistance measured using EIS is not equal to that by DC discharging, perhaps because of testing error in low frequency during the EIS testing process. However, the ohmic resistances of unit cell 1 and repeating unit 1 slightly change with increasing operation time (as seen in Fig. 17), indicating a small change in the cell microstructure associated with ohmic properties during operation. The polarization resistance of unit cell 1 increases with increasing operation time, implying that the microstructure associated with polarization properties undergoes changes, such as growth of a nickel particle in the anode, as previous literature [40] has reported. The polarization resistance of repeating unit 1 increases and then decreases, perhaps due to the effect of the CCCL on the cell cathode side. Comparing the degradation results of unit cell 1 with those of repeating unit 1, the degradation of the unit cell and the repeating unit may be assumed to be independent of polarization resistance, but mainly dependent on ohmic resistance.

From Fig. 17, it is found that the ohmic resistance  $R_s$  and the polarization resistance  $R_p$  of unit cell 2 and repeating unit 2 initially increase with increasing operation time and then decrease gradually. This may be because of the significant effect of Cr on cell

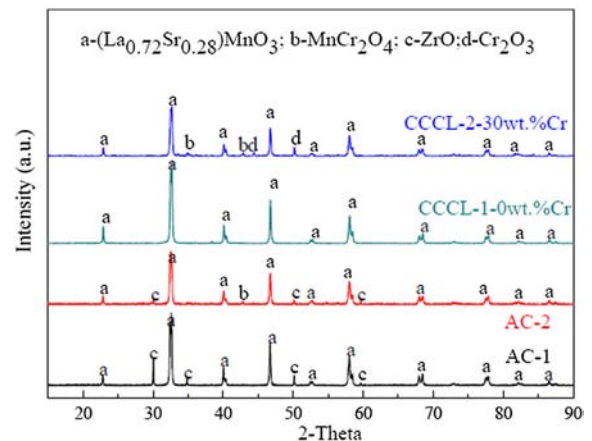


Fig. 18. XRD patterns of CCCL and the active layer in unit cells 1 and 2.

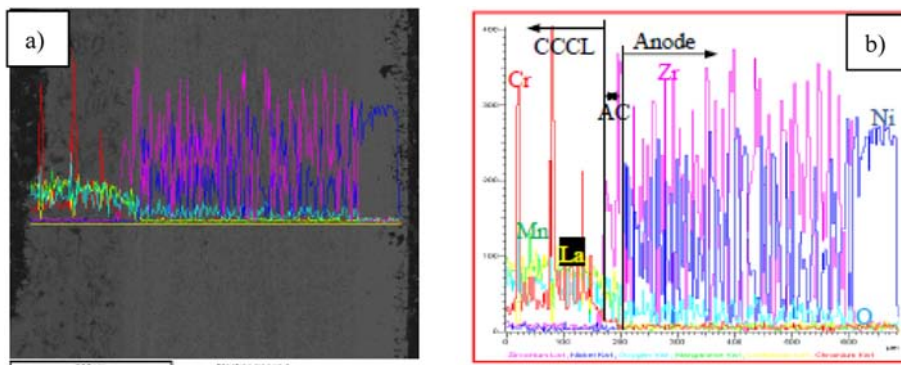


Fig. 19. Element distribution in unit cell 2.

performance during the initial operation stage, which later gradually stabilizes. This phenomenon cannot be found in the operation of unit cell 1 and repeating unit 1. The polarization resistances  $R_p$  of unit cells 1 and 2 are close to those of repeating units 1 and 2, irrespective of whether the CCCL has Cr. The ohmic resistance  $R_s$  of unit cell 1 is slightly higher than that of repeating unit 1, while the ohmic resistance  $R_s$  of unit cell 2 is slightly lower than that of repeating unit 2. These results indicate that the contact between the metal-interconnect and the cell cathode has no influence on polarization resistance, but does affect ohmic resistance. The addition of Cr in the CCCL will not increase the contact resistance between the interconnect and the cathode, but will increase the polarization and ohmic resistances of the unit cell. Comparing the results in Fig. 16b) with those in Fig. 17, the polarization resistances of the unit cell and the repeating unit inside the stack are again not a factor in cell degradation, unlike ohmic resistances of the unit cell and the repeating unit inside the stack during operation.

The phase of Cr in the cathode side of unit cells 1 and 2 is characterized by X-ray diffraction (XRD, D8 Advance, Bruker AXS), and the results are shown in Fig. 18. The composition in the CCCL of unit cell 1 is mainly  $(La_{0.72}Sr_{0.28})MnO_3$ , which is slightly different from the nominal composition of  $(La_{0.75}Sr_{0.25})_{0.95}MnO_3$ . The phase of  $MnCr_2O_4$  is also found in the CCCL of unit cell 2, but not in the composition found in the cathode side of unit cell 1, a result which is in agreement with that reported in the literature [41,42]. Therefore, elemental Cr reacts with elemental Mn to form a new phase in the actual operation of the SOFC stack. In addition, a large amount of  $Cr_2O_3$  appears in the CCCL of unit cell 2, as shown in Fig. 18. Accordingly, Cr in the cathode side exists in the phases of  $MnCr_2O_4$  and  $Cr_2O_3$ . The XRD results show that no phase of Cr appears in the active cathode of unit cell 2, due to two factors, namely, the amount of Cr in the active layer is too low for characterization by XRD, either no Cr or only a small amount of Cr is diffused into the active layer from the CCCL.

Hence, energy dispersive spectrometry (EDS) was applied to characterize Cr in the CCCL, as shown in Fig. 19. The result shows that the peak curve of Cr in the CCCL appears strong, while the distribution curve of elemental Cr in the active layer flattened immediately, indicating little or no Cr in the active layer on the cathode side. The ICP-ASE measurement indicates the presence of about a 0.25 wt. % Cr in the total amount existing in the active layer. Also, no obvious accumulation of Cr appears in the triple-boundary interface between the active layer and the electrolyte. This finding reveals that Cr deposition in the triple-boundary interface is not the only factor affecting cell performance by poisoning the cathode during stack operation, and Cr in the CCCL and in the active layer and reaction of cathode with Mn also play an important role.

#### 4. Conclusions

The MOPDs of the unit cell and the repeating unit inside the stack decrease with increasing Cr content, when Cr deposition in the CCCL of the LSM is higher than  $253.81 \mu\text{g cm}^{-2}$ . Cr exhibits seemingly no influence on the MOPD of the unit cell inside the stack where the content of Cr is less than  $253.81 \mu\text{g cm}^{-2}$ . The MOPD of the repeating unit with Cr in the CCCL is lower than that of the repeating unit without Cr. The degradation rate of the repeating units inside the stack increases with increasing Cr content, except that of repeating unit 2. Cr apparently has no influence on cell degradation when the content of Cr is less than  $182.22 \mu\text{g cm}^{-2}$ , while the cell degradation increases with increasing Cr content when Cr content is higher than  $182.22 \mu\text{g cm}^{-2}$ .

The resistance sources of the CCCL and the contact between the electrode and the interconnect increase significantly when Cr is added into the CCCL during the initial stage of the stack operation. The contact resistance between the electrode and the interconnect remains stable with increasing operation time. Cr mainly affects cell degradation with increasing operation time. The results in this study also show that cell degradation is dependent on ohmic resistance, and independent of polarization resistance. The addition of Cr in the CCCL mainly increases the ohmic resistance of the unit cells, and exhibits only slight influence on cell polarization resistance. Cr appears in phases of  $MnCr_2O_4$  and  $Cr_2O_3$  during stack operation. A small amount of Cr diffuses into the active layer on the cathode side from the CCCL, and no significant accumulation of Cr is found in the triple-boundary interface. The results indicate that Cr deposition in the triple-boundary interface is not the only factor affecting cell performance by poisoning the cathode during stack operation. The presence of Cr in the CCCL and in the active layer and the reaction of cathode with Mn are also important factors affecting cell performance.

#### Acknowledgment

The author would like to thank the financial support from National High-Tech Research and Development Program of China (863 Project No. 2009AA05Z122), China Postdoctoral Science Foundation (2012M521208) and Zhejiang Provincial Advanced Postdoctoral Scientific Program (Bsh1201010).

#### References

- [1] N.Q. Minh, *Solid State Ionics* 174 (2004) 271–277.
- [2] H.Y. Tu, U. Stimming, *J. Power Sources* 127 (2004) 284–293.
- [3] A. Hauch, P.S. Jørgensen, K. Brodersen, M. Mogensen, *J. Power Sources* 196 (2011) 8931–8941.
- [4] T. Suzuki, M. Awano, P. Jasinski, V. Petrovsky, H.U. Anderson, *Solid State Ionics* 177 (2006) 2071–2074.

- [5] H. Yokokawa, H.Y. Tu, B.I. Andreas Mai, J. Power Sources 182 (2008) 400–412.
- [6] M. Stanislawski, J. Froitzheim, L. Niewolak, W.J. Quadackers, K. Hilpert, T. Markus, L. Singheiser, J. Power Sources 164 (2007) 578–589.
- [7] N. Shaigan, W. Qu, D.G. Ivey, W.X. Chen, J. Power Sources 195 (2010) 1529–1542.
- [8] O. Thomann, M. Pihlatie, J.A. Schuler, O. Himanen, J. Kiviahio, ECS Trans. 35 (2011) 2609–2616.
- [9] S.P.S. Badwal, R. Deller, K. Fogera, Y. Ramprakash, J.P. Zhang, Solid State Ionics 99 (1997) 297–310.
- [10] S.P. Jiang, J.P. Zhang, K. Fogger, J. Electrochem. Soc. 147 (2000) 3195–3205.
- [11] K. Fujita, K. Ogasawara, Y. Matsuzaki, T. Sakurai, J. Power Sources 131 (2004) 261–269.
- [12] S.C. Paulson, V.I. Birss, J. Electrochem. Soc. 151 (2004) A1961–A1968.
- [13] M. Stanislawski, E. Wessel, K. Hilpert, T. Markus, L. Singheiser, J. Electrochem. Soc. 154 (2007) A295–A306.
- [14] S.L. Wang, M.F. Liu, Y.C. Dong, K. Xie, X.Q. Liu, G.Y. Meng, Mater. Res. Bull. 43 (2008) 2607–2616.
- [15] J. Malzbendera, P. Batfalsky, R. Vaßen, V. Shemet, F. Tietz, J. Power Sources 201 (2012) 196–203.
- [16] C. Gindorf, L. Singheiser, K. Hilpert, Steel Res. 72 (2001) 528–533.
- [17] J.A. Schuler, P. Tanasini, A. Hessler-Wyser, J.V. herle, Scripta Mater. 63 (2010) 895–898.
- [18] M. Casteel, D. Lewis, P. Willson, M. Alinger, Int. J. Hydrogen Energy 37 (2012) 6818–6829.
- [19] N.H. Menzler, I. Vinke, H. Lippert, ECS Trans. 25 (2009) 2899–2908.
- [20] J.A. Schuler, Z. Wuillemin, A. Hessler-Wyser, C. Comminges, N.Y. Steiner, J.V. herle, J. Power Sources 211 (2012) 177–183.
- [21] J.A. Schuler, C. Gehrig, Z. Wuillemin, et al., J. Power Sources 196 (2011) 7225–7231.
- [22] L.G.J. de Haart, J. Mouglin, O. Posdziech, J. Kiviahio, N.H. Menzler, Fuel Cells 09 (2009) 794–804.
- [23] W.B. Guan, L. Jin, X. Ma, W.G. Wang, Fuel Cells 12 (2012) 1085–1094.
- [24] T. Horita, D.H. Cho, F.F. Wang, T. Shimonosono, H. Kishimoto, K. Yamaji, M.E. Brito, H. Yokokawa, Solid State Ionics 225 (2012) 151–156.
- [25] K. Hilpert, D. Das, M. Miller, D.H. Peck, R. Weiss, J. Electrochem. Soc. 143 (1996) 3642–3647.
- [26] Y. Matsuzaki, I. Yasuda, J. Electrochem. Soc. 48 (2001) A126–A131.
- [27] S.P. Jiang, J.P. Zhang, Y.D. Zhen, Mater. Sci. Eng. B 119 (2005) 80–86.
- [28] S.P. Jiang, J.P. Zhang, L. Apateanu, K. Fogger, J. Electrochem. Soc. 147 (2000) 4013–4022.
- [29] S.P. Jiang, J.P. Zhang, X.G. Zheng, J. Eur. Ceram. Soc. 22 (2002) 361–373.
- [30] S.P. Jiang, J.P. Zhang, Y.D. Zhen, J. Mater. Res. 20 (2005) 747–758.
- [31] S.P. Jiang, J.P. Zhang, K. Fogger, J. Electrochem. Soc. 148 (2001) C447–C455.
- [32] J.W. Fergus, Int. J. Hydrogen Energy 32 (2007) 3664–3671.
- [33] M. Kornely, N.H. Menzler, A. Weber, E.I. Tiffée, Fuel Cells 00 (2013), 00–00.
- [34] T.S. Li, H. Miao, T. Chen, W.G. Wang, C. Xu, J. Electrochem. Soc. 156 (2009) B1383–B1388.
- [35] W.B. Guan, H.J. Zhai, L. Jin, C. Xu, W.G. Wang, Fuel Cells 12 (2012) 24–31.
- [36] L. Jin, W.B. Guan, J.Q. Niu, X. Ma, W.G. Wang, J. Power Sources 240 (2013) 796–805.
- [37] S.Q. Yang, T. Chen, Y. Wang, Z.B. Pen, W.G. Wang, Int. J. Electrochem. Sci. 8 (2013) 2330–2344.
- [38] W.B. Guan, H.J. Zhai, L. Jin, T.S. Li, W.G. Wang, Fuel Cells 11 (2011) 445–450.
- [39] J.X. Wang, Y.K. Tao, J.S. Shao, W.G. Wang, J. Power Sources 186 (2009) 344–348.
- [40] J.S. Cronin, J.R. Wilson, S.A. Barnett, J. Power Sources 196 (2011) 2640–2643.
- [41] T. Horita, Y.P. Xiong, K. Yamaji, J. Power Sources 118 (2003) 35–43.
- [42] H. Kurokawa, K. Kawamura, T. Maruyama, Solid State Ionics 168 (2004) 13–21.